Astron. Astrophys. 335, 351–362 (1998)

ASTRONOMY AND ASTROPHYSICS

Orbital evolution of asteroidal fragments into the ν_6 resonance via Yarkovsky effects

D. Vokrouhlický[1] **and P. Farinella**[2]

[1] Institute of Astronomy, Charles University, V Holešovičkách 2, CZ-180 00 Prague 8, Czech Republic
(e-mail: vokrouhl@mbox.cesnet.cz)
[2] Gruppo di Meccanica Spaziale, Dipartimento di Matematica, Università di Pisa, Via Buonarroti 2, I-56127 Pisa, Italy
(e-mail: paolof@dm.unipi.it)

Received 28 September 1997 / Accepted 24 February 1998

Abstract. We analyze the dynamical evolution of asteroidal fragments released in the Flora region, near the inner edge of the main asteroid belt, and drifting into the ν_6 secular resonance due to Yarkovsky non-gravitational effects. We find that fragments 5 to 20 m in size evolve under the "seasonal" Yarkovsky effect which causes a secular semimajor axis decay; they reach ν_6 after a time shorter than their collisional lifetime when they start within about 0.05 to 0.2 AU out of the resonance. Metal-rich fragments drift slower but have have much longer lifetimes than stony ones, so they drift farther from their formation site and sample a wider portion of the inner belt. Fragments around 100 m in size are mainly influenced by the "diurnal" Yarkovsky effect if their surface is covered by a (thin) regolith layer; this causes a random walk in semimajor axis controlled by impacts which reorient the spin axis. Within their lifetime of ≈ 100 Myr these fragments can move throughout the inner part of the asteroid belt, episodically crossing ν_6. Meter-sized stony fragments, which probably deliver most meteorite falls, may also drift into the resonance under the "diurnal" effect, provided their surfaces have low thermal conductivities and/or their rotation is unusually slow. According to our dynamical model, which is truncated to $15^{\rm th}$ degree in the fragment's orbital eccentricity, ν_6 resonance effects typically result into large eccentricity increases, such that main-belt orbits rapidly become Earth-crossing when the resonance is reached and/or crossed. This confirms the idea that the interplay of resonant dynamics and Yarkovsky-related semimajor axis mobility is crucial in the transport of meteorites and small near-Earth asteroids from the main asteroid belt to the near-Earth space.

Key words: celestial mechanics, stellar dynamics – minor planets, asteroids – meteors, meteoroids

1. Introduction

The Earth permanently experiences the infall of interplanetary matter, a large fraction of which origins in the main asteroid belt. Because of the relatively frequent collisions there, this source population spans all possible values of masses and sizes, with a characteristic quasi-power-law distribution (Dohnanyi 1969, Campo Bagatin et al. 1994). Whereas most meteorites appear to be delivered by pre-atmospheric bodies of the order of 0.1 to 1 m in size, occasional bright bolides reach several meters, and according to Ceplecha (1992, 1996) a clear maximum of the incoming mass versus size curve is present at a size of 10–20 m. These objects have been recently observed also in near-Earth space (Rabinowitz et al. 1993, Rabinowitz 1994) and while exploding in the high atmosphere (Tagliaferri et al. 1994). For Tunguska-like impactors 50–100 m in diameter, only one event per 100–1000 yr is expected, but extensive disruption on the ground is engendered. Therefore, for a number of different reasons it is important to understand the dynamical mechanisms which are involved in transferring from the main belt objects of sizes between ≈ 0.1 and 100 m – especially if, as we will argue in this paper, these dynamical mechanism are somewhat different from those relevant for larger asteroids.

The standard way of solving the problem of how material is transported from the asteroid belt to the Earth resorts to the peculiar dynamical evolution of bodies once they get close to or inside the main mean motion and/or secular resonances with the planets. Fragments from asteroidal collisions undergo orbital velocity changes of the order of 100 m/s, and as a result the orbits of some of them are injected into the resonances starting from the nonresonant orbits of their parent bodies (Farinella et al. 1993a, 1994a). Subsequently, as a consequence of resonant gravitational perturbations by the giant planets, the orbital eccentricity grows to values (≈ 0.6) allowing Earth crossing within only a few Myr, and then the interplay of resonant effects and planetary encounters drives the bodies to hit the Sun or the planets, or to be ejected from the Solar System by Jupiter (Farinella et al. 1993b, 1994b; Froeschlé et al. 1995; Jopek et al. 1995; Migliorini et al. 1997; Gladman et al. 1997).

However, it has been realized recently that, at least for meteorite-sized (≈ 0.1 to 10 m) bodies, this cannot be the whole story. While in interplanetary space, meteorites are exposed to cosmic radiation (provided they lay within about 1 m from the surface of the body carrying them), and measurements of these cosmic-ray exposure (CRE) ages give values between 5 and

Send offprint requests to: D. Vokrouhlický

50 Myr for most stony meteorites, and about 10 times as long for iron-rich meteorites. Since these ages are much longer than the dynamical transfer times through the resonances, and also than the typical lifetimes of near-Earth objects (≈ 10 Myr, according to Gladman et al. 1997), one must assume that asteroid fragments typically spend relatively long times in nonresonant main-belt orbits before being transferred to the near-Earth space. As we have recently pointed out (Hartmann et al. 1997, Farinella et al. 1997, 1998), a non-gravitational dynamical mechanism allowing for such a slow drift of small bodies through the asteroid belt before "falling" into the resonances is known since a long time: it is the so-called *Yarkovsky effect*.

This effect is a recoil force due to radiation pressure, arising whenever a spinning body re-emits anisotropically the absorbed solar radiation. As shown by a number of authors (Öpik 1951; Radzievskii 1952; Peterson 1976; Afonso et al. 1995; Rubincam, 1995, 1998; Farinella et al. 1998), it can cause significant long-term semimajor axis effects on asteroid fragments in the size range from about 0.1 to 100 m (smaller bodies are more affected by other non-gravitational forces, see Burns et al. 1979, while larger ones have a too small area-to-mass ratio). In particular Farinella et al. (1998) have recently shown that, depending on the size, rotational state and thermal properties of the fragment, two different variants of the Yarkovsky effect may play a dominant role: a "diurnal" effect, which is more important for slowly rotating, low-obliquity, regolith-covered fragments; and a "seasonal" effect, favoured for high-obliquity, fast rotators with a lower (bare-rock) surface thermal inertia. Whereas the latter effect always causes a secular, drag-like decrease of the orbital semimajor axis, the former one may result into either positive or negative semimajor axis changes, depending on the sense of rotation; in all cases, the amplitude of the semimajor axis effect depends on the obliquity angle. If collisions change frequently enough and in random way the orientation of the spin axis, the Yarkovsky-driven semimajor axis drift also undergoes stochastic variations in rate. These peculiarities make a realistic modelling of the orbital evolution of small asteroid fragments much more complicated than in the case of larger bodies, for which gravitational forces alone are important.

In this paper we intend to start a detailed, realistic study of how the Yarkovsky effect can interact with resonant N-body dynamics in transporting small asteroid fragments to the near-Earth region. We will deal in particular with objects originating in the so-called Flora region, in the inner part of the main asteroid belt, and drifting into the ν_6 secular resonance, which corresponds to the inner edge of this zone at a semimajor axis slightly exceeding 2 AU. In the last decade several studies have addressed the purely gravitational dynamics of bodies located in the ν_6 resonance (Froeschlé and Scholl 1987; Yoshikawa 1987; Scholl and Froeschlé 1991; Morbidelli and Henrard 1991; Morbidelli 1993; Valsecchi et al. 1995) or injected into it as a result of collisions in the neighboring Flora region of the main belt (Farinella et al. 1993a,b; Morbidelli et al. 1994). However, little is known about the effectiveness of this resonance in pumping up the orbital eccentricity in the presence of dissipative, non-gravitational perturbations such as the Yarkovsky force.

Therefore, our aim here is that of presenting a relatively simple model for the orbital evolution of asteroidal fragments in the region of the orbital element space close to the ν_6 resonance, under the simultaneous influence of the gravitational perturbations by the major planets and the Yarkovsky thermal effects. In order to better understand the significance of our results, we have decided to keep our model analytical as far as possible for the time being. Thus, we average analytically the gravitational perturbing function and integrate numerically the averaged system of Lagrange equations only. Moreover, due to the complexity of the thermal effects, we consider only their most important orbital effect, namely the secular changes in semimajor axis, neglecting their influence on other orbital elements. This is certainly a crude approximation, as Rubincam (1995, 1998) and Vokrouhlický and Farinella (1998) have showed that Yarkovsky effects can lead to significant long-term changes in the eccentricity and inclination as well.

The remainder of this paper is organized as follows. Sect. 2 is devoted to a description of our dynamical model, for both the gravitational (Sect. 2.1) and non-gravitational (Sect. 2.2) perturbations. In Sect. 3 we present some tests of the corresponding theory compared to direct numerical integrations and other results, and then we discuss a number of runs for different model populations of bodies, for which either the "seasonal" or the "diurnal" Yarkovsky effects play a dominant role. In Sect. 4 we discuss the significance of these results for our understanding of the delivery of small asteroid fragments and meteorites to the near-Earth space.

2. Dynamical model

2.1. Secular perturbations by the outer planets

As a first step we are going to summarize our analytical model for the secular influence of the major planets, Jupiter and Saturn, on the fragment's orbit. Following the formalism of planetary theories such as those of Duriez (1977) and Laskar (1985), we introduce the pair of complex, non-singular mean orbital elements (ζ, ξ) defined as

$$\zeta = k + \imath h = e \exp(\imath \varpi) , \tag{1}$$

$$\xi = q + \imath p = \sigma \exp(\imath \Omega) , \tag{2}$$

where e is the mean eccentricity e, $\varpi = \Omega + \omega$ the mean argument of pericenter, $\sigma = \sin I/2$, I being the mean inclination, and $\imath = \sqrt{-1}$. Then, the secular evolution of the orbit is determined by the set of differential equations

$$D\zeta = \frac{1}{na^2}\left[2\eta\frac{\partial R}{\partial \bar{\zeta}} + \frac{\zeta}{\eta}\mathrm{Re}\left(\xi\frac{\partial R}{\partial \xi}\right)\right] , \tag{3}$$

$$D\xi = \frac{1}{na^2}\left[\frac{1}{2\eta}\frac{\partial R}{\partial \bar{\xi}} + \frac{\xi}{\imath\eta}\mathrm{Im}\left(\zeta\frac{\partial R}{\partial \zeta}\right)\right] \tag{4}$$

(see Laskar 1985), where $D = -\imath d/dt$, $\eta = \sqrt{1-e^2} = (1-\zeta\bar{\zeta})^{1/2}$, a is the mean semimajor axis, n the mean motion ($n^2a^3 = Gm_\odot$, $m_\odot$ being the solar mass). Overbarred quantities are complex conjugates, while Re and Im denote the

real and imaginary parts of a complex quantity, respectively. The function R in Eqs. (3) and (4) is the secular part of the planetary perturbing function. In our approximate model, we adopt the two following simplifications:

1. we neglect the inclinations of the perturbing planets ($\xi' = 0$) and take into account only their eccentricities ($\zeta' \neq 0$; planetary variables are primed);
2. we adopt a linear approximation for the averaged (secular) perturbing function, neglecting quadratic and higher order terms in the planetary masses.

In this case, it is well known (see e.g. Brouwer and Clemence 1961) that the disturbing function R is due to the direct part of the planetary perturbation only, and reads

$$R = \left[\frac{Gm'}{|\mathbf{r}-\mathbf{r}'|}\right]_{\rm sec} = \frac{Gm'}{a'}\sum_{i\in\mathbf{Z}^6}\phi_i(\alpha)\xi^{2i_1}\bar{\xi}^{2i_2}\zeta^{i_3}\bar{\zeta}^{i_4}\zeta'^{i_5}\bar{\zeta}'^{i_6} , \quad (5)$$

where i denotes the vector of indexes $(i_1, i_2, ..., i_6)$, m' and a' are the planet's mass and semimajor axis (a sum over the two considered planets is implicit), and α is the ratio between the fragment's and planet's semimajor axes. Taking into account the specific problem we are dealing with (fragments with $a \approx 2$ AU and e up to ≈ 0.7), we have expanded the perturbing potential (5) to a high order in the fragment's eccentricity. By using the algebraic manipulator MINIMS, developed by M. Moons at the University of Namur (Moons 1991), we have computed all terms with indexes $|i_3|+|i_4| \leq 15$ and $|i_1|+|i_2|+|i_5|+|i_6| \leq 3$. In other words, the disturbing function has been developed up to the fifteenth degree in the fragment's eccentricity. The second condition means that we have kept a lower number of terms in the fragment's inclination, namely those up to $\sin^6 I/2$ (included) only.

The $\phi_i(\alpha)$ factors in Eq. (5) can be expressed as functions of the Laplace coefficients and their derivatives. Because of the specific character of our application, with secular changes in the fragment's semimajor axis, we have calculated all these terms with particular care analytically. Starting from the formulæ for the lowest order Laplace coefficients (Brouwer and Clemence 1961):

$$b^{(0)}_{1/2}(\alpha) = \frac{4}{\pi}K(\alpha) , \quad (6)$$

$$b^{(1)}_{1/2}(\alpha) = \frac{4}{\pi}\frac{K(\alpha)-E(\alpha)}{\alpha} , \quad (7)$$

with $K(\alpha)$ and $E(\alpha)$ denoting the complete elliptic integrals of the first and second kind, we have

$$b^{(j)}_{s+1/2}(\alpha) = \alpha^J w^{2s}(\alpha)\left[P^j_s(\alpha)b^{(0)}_{1/2}(\alpha) + Q^j_s(\alpha)b^{(1)}_{1/2}(\alpha)\right] , \quad (8)$$

where $J = \min(0, 1-j)$ and $w(\alpha) = 1/(1-\alpha^2)$. Recurrence formulæ for the polynomials $P^j_s(\alpha)$ and $Q^j_s(\alpha)$ are given by Šidlichovský and Melendo (1986) or Šidlichovský (1989; alternatively, see Laskar 1991). The derivatives of the Laplace coefficients (8) can then be computed by simple algebra.

The structure of the eccentricity Eq. (3) can be schematically written as

$$D\zeta = g\left(a, e^2, \sigma^2\right)\zeta + f\left(a, e^2, \sigma^2\right)\zeta' + \text{other nonlinear terms} , \quad (9)$$

where g and f are known functions. As for the long-term evolution of the planetary orbits, we have used the Laplace-Lagrange secular solution with numerical coefficients given by Knežević (1986). Jupiter's and Saturn's complex eccentricities are thus given by the simple harmonic development

$$\zeta' = \sum A_j \exp \imath\left(g_j t + \phi_j\right) , \quad (10)$$

with constant coefficients. In our case, the most important of these constants is $g_6 = 27.''360\ \mathrm{yr}^{-1}$; this value, derived by Knežević (1986), is in good agreement with numerical determinations of the corresponding frequency (Laskar 1988; Nobili et al. 1989); as we will see in Sect. 3.1, our results are not sensitive to small changes in this value. The structure of Eqs. (9) and (10) shows that the linear solution of these equations has a singularity when $g\left(a, e^2, \sigma^2\right) = g_6$: of course this is the well-known condition for the ν_6 resonance, which is located near the inner edge of the main asteroid belt.

We have not taken into account the influence of the inner planets for several reasons. On one hand, we have chosen to develop an analytical model, and it is well known (see e.g. Hagihara 1971) that classical developments of the planetary perturbing potential in the form (5) suffer divergencies whenever the minor body can cross the orbit of a planet. As we shall see, crossing the ν_6 resonance typically leads to high-eccentricity orbits, which cross those of both Mars and the Earth, and therefore analytical developments of type (5) would be useless if we wanted to include these planets. On the other hand, we believe that the main conclusions of our work would not be altered by the inclusion of the gravitational influence of the inner planets, because (i) the corresponding shift in the position of ν_6 is small (Knežević et al. 1991); (ii) mean motion and secular resonances with the inner planets can be effective only for semimajor axes smaller than 2 AU (Milani et al. 1989, Michel 1997); and (iii) close encounters with Mars do not affect much the orbital evolution of bodies which are being transported from the main asteroid belt to the near-Earth zone (Gladman et al. 1997).

2.2. Thermal perturbations of the fragment's orbit

Besides the gravitational effects, and as a major novelty of this work, we include in our model a simplified treatment of the thermal Yarkovsky effects acting on small asteroidal fragments, by taking into account the corresponding secular changes in semimajor axis. A complete theory for the orbital perturbations due to the Yarkovsky force is fairly complex, since the intensity of the force at a given time depends on the thermal state of the body, that is on the thermal inertia and the insolation the body has received over a time of the order of a rotation (for the "diurnal" effect) or orbital period (for the seasonal one); hence, at

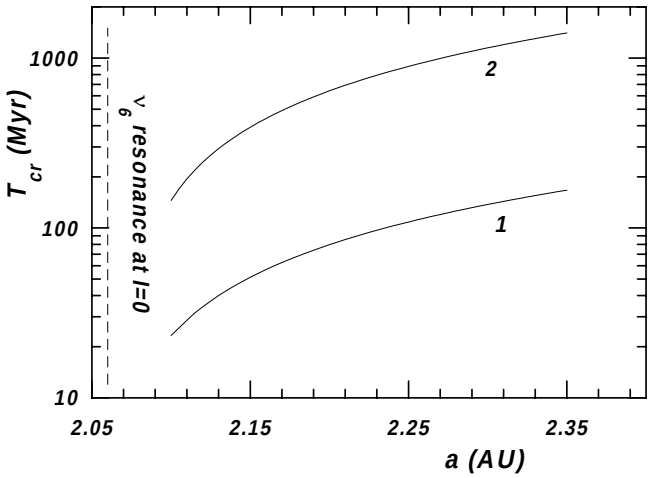

Fig. 1. Diffusion time T_{cr} (in Myr) required for reaching the ν_6 resonance at zero inclination vs. initial semimajor axis a (in AU). Two types of objects are assumed to evolve under the Yarkovsky "seasonal" effect: (i) $R = 5$ m basalt fragments (curve 1), and (ii) R=10 m iron-rich bodies (curve 2).

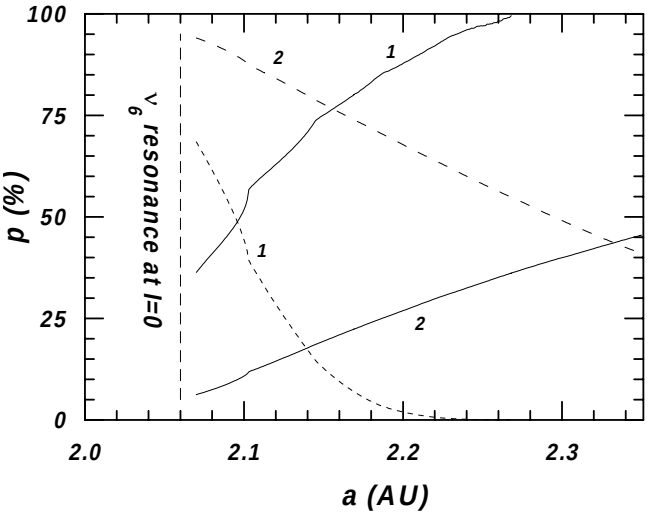

Fig. 2. Diffusion of regolith-covered stony objects 50 m in radius under the "diurnal" Yarkovsky effect, taking into account the random reorientation of spin axes caused by impacts (assumed to occur at typical intervals $\tau_{rot} = 24$ Myr). The initial semimajor axes values (in AU) are given on the horizontal axis. The full lines give the average percentage of a collisional lifetime τ_{disr} required to reach ν_6 and the dashed lines the percentage of bodies reaching the resonance before being disrupted. Curves 1 and 2 were derived assuming $\tau_{disr} = 140$ Myr (according to Farinella et al. 1998) and $\tau_{disr} = 4$ Byr, respectively.

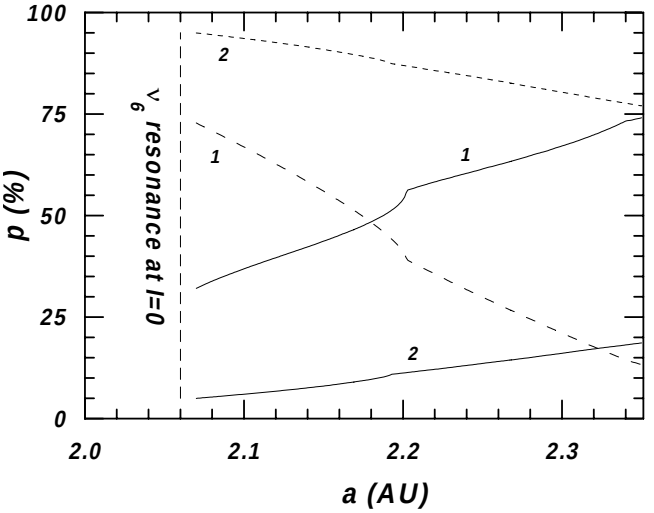

Fig. 3. The same as Fig. 2 but for objects 1 m in radius. Curves 1 correspond to stony bodies, with $\tau_{rot} = 3.3$ Myr and $\tau_{disr} = 20$ Myr; curves 2 correspond to iron bodies, with $\tau_{rot} = 7$ Myr and $\tau_{disr} = 1.4$ Byr (Farinella et al. 1998).

least in the "seasonal" case, the Yarkovsky force depends in a complex way on the orbital elements. In the current context, in order to keep the problem tractable, we just simulate the secular semimajor axis effects by adding a simple linear term in the semimajor axis of the fragment's orbit, that is assuming that $a(t) \simeq a(0) + \dot{a}\, t$. The value of the semimajor axis rate $\dot{a}$ is in principle determined by a number of different circumstances. As we mentioned in Sect. 1, in the case of the "seasonal" version of the Yarkovsky effect the sign of $\dot{a}$ is always negative, while in the case of of the "diurnal" version it can be either positive or negative, according to the orientation of the spin axis. In quantitative terms, we are going to use the results of Farinella et al. (1998). For the reasons discussed in that paper, we assume that the rotation rate of asteroid fragments is inversely proportional to their size, with 1 km diameter bodies spinning in 5 hr.

The "seasonal" effect is the dominant one for regolith-free fragments of size of the order of 10 m. For this case, we adopt the following empirical model:

$$\dot{a} \simeq -\,\dot{a}_{\max}(\Theta_n, R, a)\,\sin^2\gamma\;, \tag{11}$$

where γ is the obliquity of the fragment's polar axis (that is, the angle between the spin axis and the normal to the mean orbit), a is the semimajor axis and Θ_n is a thermal inertia parameter related to temperature changes with periodicities of the order of the orbital period. The dependence of the amplitude $\dot{a}_{\max}$ on a, on the body's (mean) radius R and on the Θ_n parameter is quite complex (see Farinella et al. 1998, Rubincam 1998), so we just use the following typical values, consistent with the results of the above-mentioned papers for $R = 5$ m and at an orbital semimajor axis $a \approx 2$ AU: $\dot{a}_{\max} \simeq 3.7 \times 10^{-3}$ AU/Myr for stony fragments and $\dot{a}_{\max} \simeq 4.2 \times 10^{-4}$ AU/Myr for iron-rich objects. If one assumes a frequent enough collisional reorientation of the spin axis (with all directions being equally likely), the average drift rate is reduced by a factor $2/3$ with respect to $\dot{a}_{\max}$.

As for the "diurnal" Yarkovsky effect, which is probably the dominant one for meter-sized bodies and for relatively large ($R \simeq 25 - 100$ m) regolith-covered fragments, we use

$$\dot{a} \simeq \dot{a}_{\max}\, f\,(\Theta_\omega, R, a)\,\cos\gamma\;, \tag{12}$$

where Θ_ω is the thermal parameter related to temperature changes over times comparable to the spin period. In this case

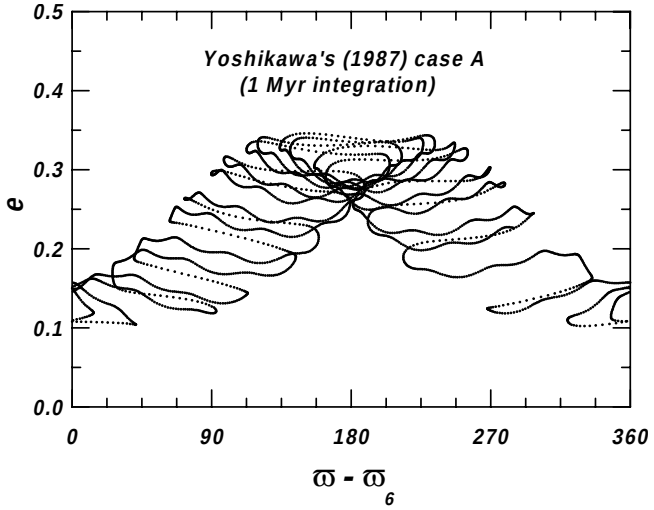

Fig. 4. Mean eccentricity e vs. the critical argument of the ν_6 resonance $\varpi - \varpi_6$ (with $\varpi_6 = g_6 t + \mathrm{constant}$), for initial conditions corresponding to Yoshikawa's (1987) case A test body. The plot shows the orbital evolution over a time span of 1 Myr, computed by the analytical scheme described in Sect. 2.

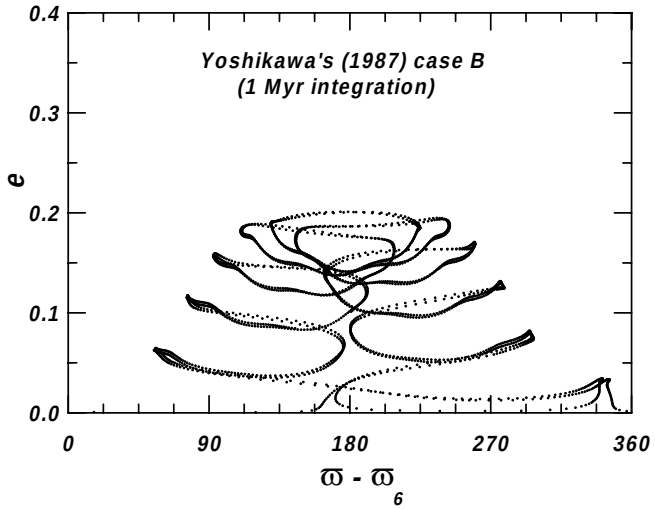

Fig. 5. The same as Fig. 3 but for Yoshikawa's (1987) case B test body.

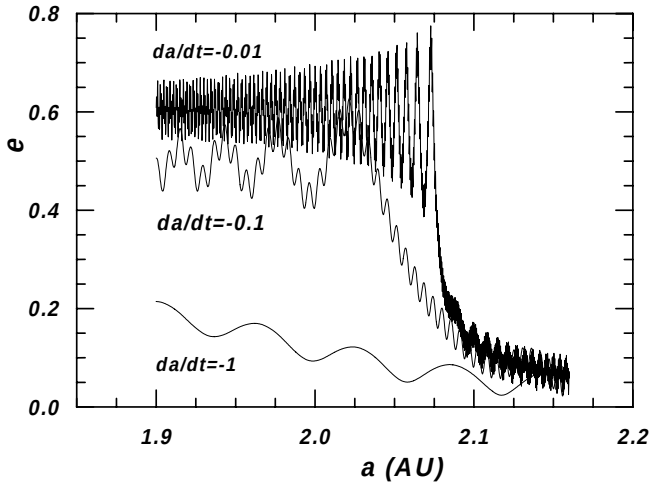

Fig. 6. Effects on the orbital eccentricity e of ν_6 resonance crossings with different semimajor axis decay rates da/dt (in AU/Myr). Higher decay rates result into a lower efficiency of the resonance in pumping up the eccentricity.

the value of $\dot{a}_{\max}$ depends sensitively on the thermal conductivity of the surface layer, as a very thin ($\approx$ 1 mm) layer of regolith-like low-conductivity material is enough to strongly affect the "diurnal" component of the surface temperature distribution. Assuming thermal properties similar to those measured for the lunar regolith (Rubincam 1995), Farinella et al. (1998) obtained in this case $\dot{a}_{\max} \simeq 2.65 \times 10^{-3}$ AU/Myr for a $R = 50$ m object and $\dot{a}_{\max} \simeq 4.52 \times 10^{-2}$ AU/Myr for $R = 1$ m. On the other hand, for bare-rock surfaces Farinella et al. (1998) used the conductivity of terrestrial basalt, which is close to the maximum values measured for chondritic meteorites (Yomogida and Matsui 1983), and this gives the much lower value $\dot{a}_{\max} \simeq 8.25 \times 10^{-4}$ AU/Myr at a radius of 1 m. For meter-sized, regolith-free iron meteorites, using the higher conductivity of metallic iron, Farinella et al. (1998) obtained $\dot{a}_{\max} \simeq 7.29 \times 10^{-5}$ AU/Myr. These estimates were always obtained at $a \approx 2$ AU.

As we explained in Sect. 1, an essential ingredient of the Yarkovsky effects is the collisional reorientation of the fragment spin axes, resulting into random changes of the obliquity angle γ. To take this into account, we can use the Farinella et al. (1998) estimates for the characteristic time between two collisions imparting to a given target an angular momentum of rotation comparable to the pre-existing one – keeping in mind that estimates of this kind are highly uncertain, owing to our poor knowledge of the small-size projectile flux in the asteroid belt. According to these estimates, the reorientation time τ_{rot} scales proportionally to $R^{1/2}$, and is ≈ 3.3, 8 and 24 Myr for fragments 1, 5 and 50 m in radius, respectively. For iron fragments, the higher density results in time scales longer by a factor of about 2.5.

In order to assess the extent of the overall semimajor axis decay in the case of the "seasonal" Yarkovsky effect and of the corresponding random walk for the "diurnal" effect, we have performed the following tests. Taking the initial semimajor axis in the range 2.1 to 2.35 AU, we have let the orbits evolve according to Eqs. (11) and (12). We have considered separately the cases of bodies dominated by the "seasonal" and "diurnal" effect: in the former case we simulated the orbital evolution of stony and iron fragments, 5 and 10 m in radius, respectively, whereas in the latter case we considered either "large" bodies, 50 m in radius, or "small", meter-sized fragments (both stones and irons). For the "diurnal" runs we always assumed that the bodies are covered by thin, regolith-like insulating layers, because otherwise the random-walk evolution is very limited (at most a few hundredths AU). In each case we performed 10^6 test runs, always reorienting the spin axis in a random direction at the typical intervals specified above.

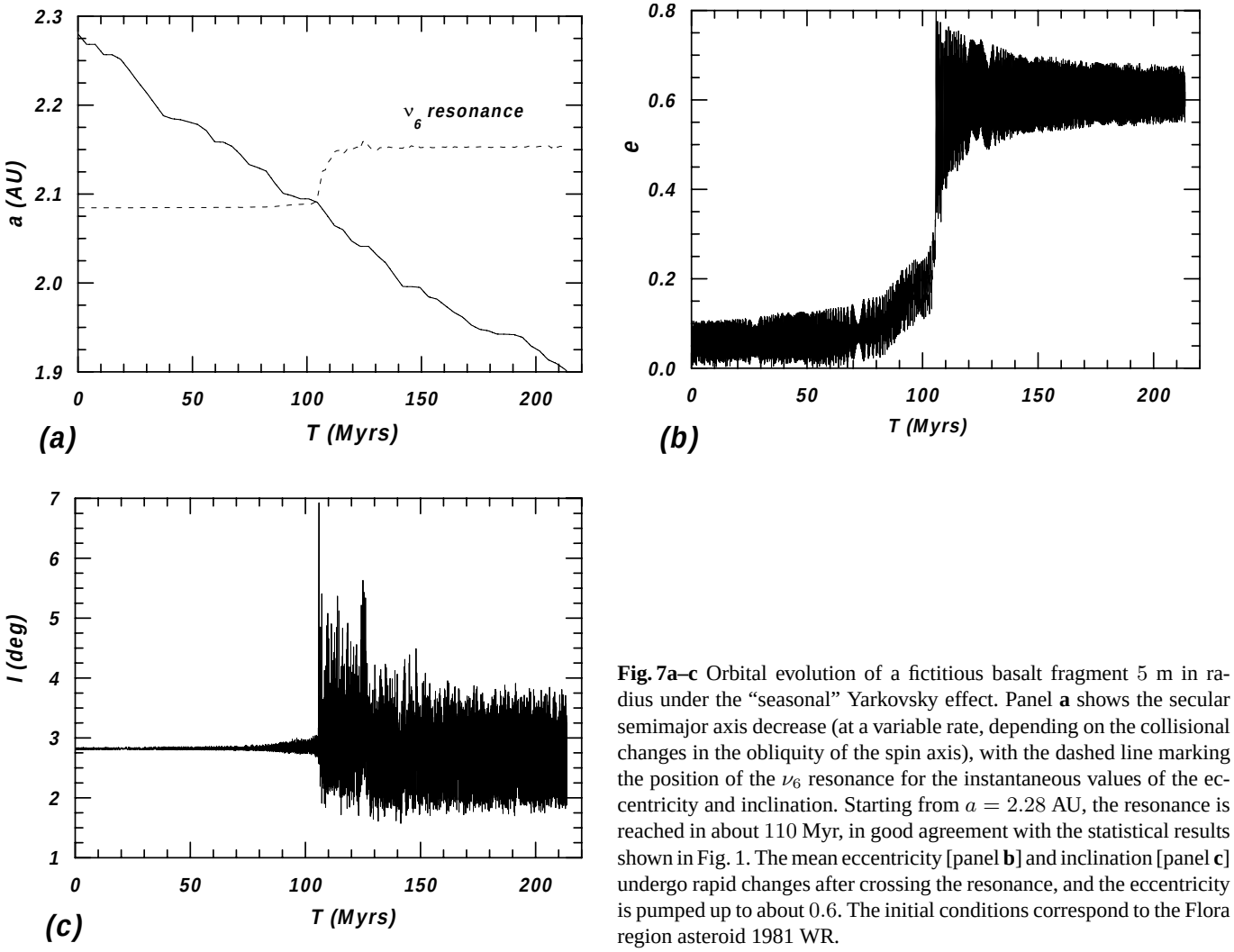

Fig. 7a–c Orbital evolution of a fictitious basalt fragment 5 m in radius under the "seasonal" Yarkovsky effect. Panel **a** shows the secular semimajor axis decrease (at a variable rate, depending on the collisional changes in the obliquity of the spin axis), with the dashed line marking the position of the ν_6 resonance for the instantaneous values of the eccentricity and inclination. Starting from $a = 2.28$ AU, the resonance is reached in about 110 Myr, in good agreement with the statistical results shown in Fig. 1. The mean eccentricity [panel **b**] and inclination [panel **c**] undergo rapid changes after crossing the resonance, and the eccentricity is pumped up to about 0.6. The initial conditions correspond to the Flora region asteroid 1981 WR.

Fig. 1 shows the mean time required for asteroid fragments drifting under the "seasonal" effect to reach the value $a = a_6 \simeq 2.06$ AU, which corresponds to the position of the ν_6 resonance for small-inclination orbits. Statistically, a 5-meter stony boulder released at the middle of the Flora region (approximately 2.25 AU) reaches the resonance in about 120 Myr, whereas a time span a factor 10 longer is necessary for iron-rich objects. We recall that, according to the estimates of Farinella et al. (1998), the typical collisional lifetimes of the two types of bodies in the main belt are of 45 Myr and 4.4 Byr, respectively. If these average lifetimes are correct, our results imply that stony fragments can reach the resonance before being shattered by impacts if they are unusually long-lived and/or they start from a semimajor axis strip of width ≈ 0.075 AU along the resonance border, whereas iron fragments may come from the whole Flora region. Thus, although iron fragments drift slower, they can drift much farther inside from their formation site as a consequence of the longer collisional lifetime. Note that the bodies discussed here are larger than the majority of meteorites, which have pre-atmospheric sizes ≈ 0.1–1 m; nevertheless, we think that they are quite relevant not only in themselves (as explained in Sect. 1), but also for meteorites, because a significant fraction of their mass lies at depths such that cosmic-ray irradiation is possible, and since many meteorites appear to have undergone complex exposure histories (Wetherill 1980), it is possible that they are just multi-generational fragments from objects several meters across.

Fig. 2 shows the results of our test runs for the larger, regolith-covered fragments whose semimajor axis undergoes a kind of random walk. Of course, only a fraction of the test bodies reaches the resonance within any given time. The two dashed lines in the figure give the fraction of bodies ending up into ν_6 within 140 Myr (which is approximately the collisional lifetime of stony objects of this size) and 4 Byr. Note that, while there is equal probability of increasing and decreasing the semimajor axis at any given instant, the probability of crossing the ν_6-resonance is greater than 50% over 4 Byr, because any excursion in semimajor axis below the critical limit $a_6 = 2.06$ AU has been classified as a resonance crossing, independently of the subsequent evolution. The full lines in Fig. 2 show the average diffusion time as a function of the starting semimajor axis. The "jumps" apparent in particular in the upper curve are related

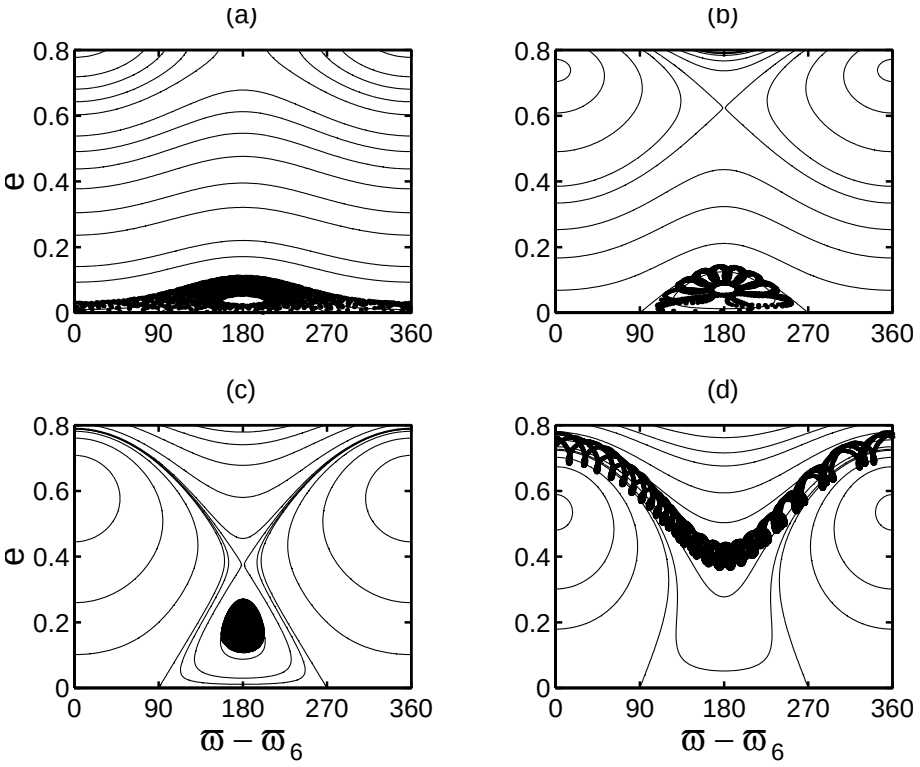

Fig. 8a–d The orbital evolution shown in Fig. 7 is shown here in the eccentricity vs. critical argument ($\varpi - \varpi_6$) plane, superimposed onto the the level curves of the averaged Hamiltonian. The four plots refer to four successive stages of the evolution, in which the semimajor axis and inclination are approximately constant. As the semimajor axis is decreased, the level curves of the Hamiltonian shift and change their topology, and as a result the orbit evolves from a low-eccentricity circulation, to a libration around $\varpi - \varpi_6 = 180^\circ$ to a high-eccentricity circulation.

to the discrete number of reorienting impacts undergone during the trip by fragments starting at different distances from the resonance. These results show that the ν_6 resonance can collect regolith-covered fragments several tens of meters in size from the whole inner part of the Flora region. Possibly this might explain why bodies in this size range appear to be overabundant in near-Earth space, compared to a power-law extrapolation from km-sized objects (Rabinowitz 1993, 1997, 1998), since the latter are not affected by non-gravitational forces in a significant way.

Fig. 3 illustrates the corresponding results for meter-sized objects. Also at this size a large fraction of asteroid fragments can reach the resonance from the Flora region within their collisional lifetime, provided they are covered by a thin insulating layer. The "jumps" are due to the same reason as for Fig. 2. Again, iron bodies are more mobile owing to their longer lifetimes. We stress that the "diurnal" Yarkovsky random walk becomes much less effective assuming a surface conductivity typical of "bare" rock or iron. For real meteorites, the situation may be in between these two extreme cases, because of the significant porosity of many meteorites (Consolmagno et al. 1998) which is likely to lower their thermal conductivity (Yomogida and Matsui, Fig. 10). Also, we have neglected the possibility that as a result of chance impacts some fragments end up spinning at rates much lower than usual (say, with a 1-hr spin period). Such slow rotators would have a "diurnal" $\dot{a}_{max}$ almost an order of magnitude larger than our nominal fast-rotating bodies (see Farinella et al. 1998, Fig. 1), and therefore some "steps" in the random walk controlled by collisions may become much larger than usual.

We note that in the models used to derive Figs. 2 and 3 we have neglected the presence of the 3:1 mean motion Jovian resonance near 2.5 AU, which would also rapidly eject any fragments inserted into it. Of course, taking into account this resonance would somewhat decrease the percentages of ν_6-reaching fragments starting from the middle and outer portions of the Flora region. On the other hand, taking into account the relatively weak dependence of the Yarkovsky effects on semimajor axis (Farinella et al. 1998), the results illustrated in Figs. 2 and 3 can be applied more or less unchanged to fragments starting near the 3:1 resonance and eventually falling into it (instead of ν_6). However, we plan to investigate in more detail the interplay of mean motion resonances and the Yarkovsky effects in a future paper.

3. Tests and results

3.1. Validation of the method

Before discussing the results of our orbital evolution runs including the Yarkovsky effects, we report on some checks that we have made to test our analytical integration scheme for the secular resonance effects.

First, we repeated several integrations performed with a fully numerical technique by Yoshikawa (1987). Figs. 4 and 5 show our results over a 1 Myr time span for Yoshikawa's fictitious test particles A and B. Comparing these plots with Yoshikawa's Figs. 9a and 9b, we observe an excellent agreement with the numerical results, at least as far as the eccentricity evolution is concerned. Actually, the situation is somewhat worse for the

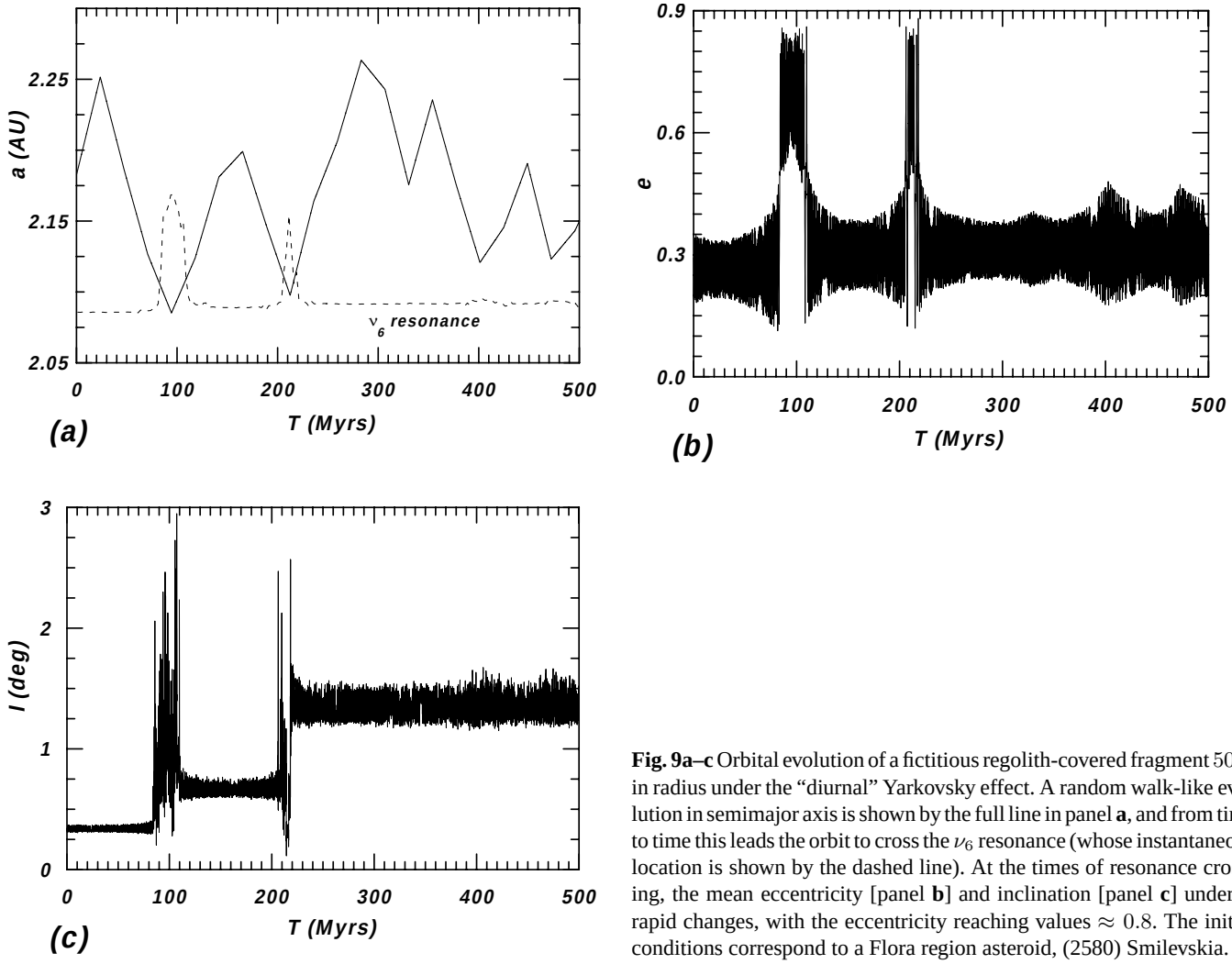

Fig. 9a–c Orbital evolution of a fictitious regolith-covered fragment 50 m in radius under the "diurnal" Yarkovsky effect. A random walk-like evolution in semimajor axis is shown by the full line in panel **a**, and from time to time this leads the orbit to cross the ν_6 resonance (whose instantaneous location is shown by the dashed line). At the times of resonance crossing, the mean eccentricity [panel **b**] and inclination [panel **c**] undergo rapid changes, with the eccentricity reaching values ≈ 0.8. The initial conditions correspond to a Flora region asteroid, (2580) Smilevskia.

inclination evolution, but this had to be expected, because we have neglected completely the planetary inclinations and have kept only a small number of terms containing the asteroid's inclination in the perturbing function (see Sect. 2). On the other hand, since we are mostly interested in the way the ν_6 resonance pumps up the eccentricity, a very accurate model for the inclination effects is not really needed.

By performing a number of tests of this kind we have become confident that our results are realistic provided the eccentricity and the inclination of the fragment's orbit do not exceed maximum values of about $0.6 - 0.7$ and $10 - 15°$, respectively. For very high eccentricities, the the results of the analytical model become unreliable (for instance, we could not reproduce the Sun-grazing dynamics described by Farinella et al. 1994b and Froeschlé et al. 1995). Also, we failed to reproduce Yoshikawa's (1987) case C test integration when the eccentricity exceeds ≈ 0.7. Actually, in this case it is mainly the inclination that undergoes large excursions (up to about $25°$) near the peak of the eccentricity cycle, and this appears to trigger an instability in our analytical results for the eccentricity. This behavior is probably related to the presence of the η factor, which becomes singular for $e \to 1$, in the denominator of Eq. (4). Overall, however, these limitations of the analytical model are not very important in the current context, since fragments injected into ν_6 become Earth-crossing for eccentricities of about 0.5, and most asteroids in the Flora region have inclinations smaller than $10°$.

As a second test, we have checked how the eccentricity evolution in crossing the ν_6 resonance is affected by different rates of the semimajor axis decay. The results are summarized in Fig. 6. The same initial conditions ($a = 2.16$ AU, $e = 0.06$, $i = 0$) have been taken in the three cases. As the decay rate $\dot{a}$ increases in magnitude (i.e., for faster crossings of the resonance), the eccentricity evolution becomes less and less sensitive to the resonance crossing. Basically, this is due to the fact that fast-decaying orbits spend shorter times in the resonance region, where planetary perturbations are effective in pumping up the eccentricity. This is a general property of resonance crossing processes due to dissipative perturbations (see e.g. Hamilton 1994, Liou and Zook 1997), and our model reproduces it very well.

Finally, we have repeated the integrations of Fig. 6 but replacing the Knežević (1986) model for the evolution of plane-

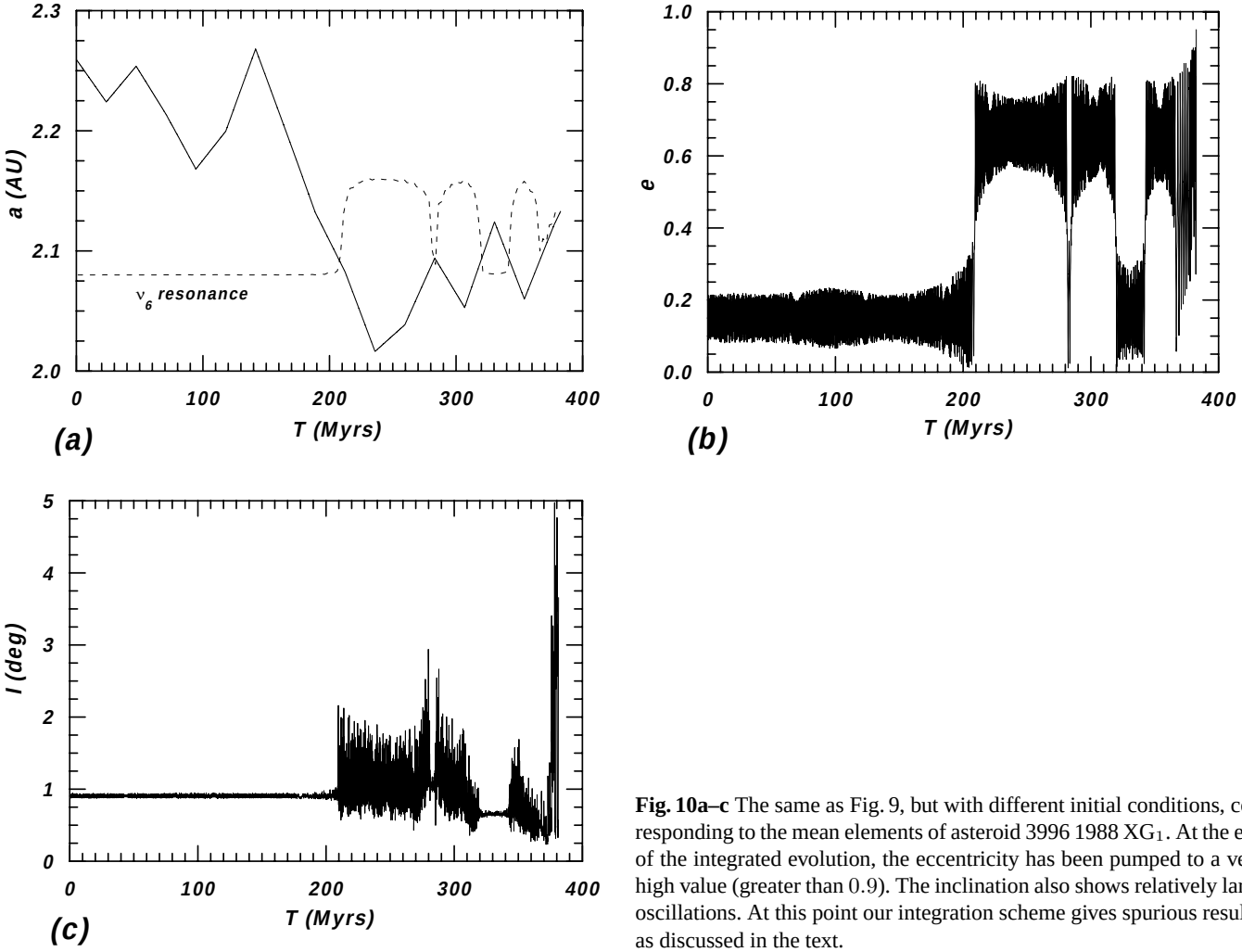

Fig. 10a–c The same as Fig. 9, but with different initial conditions, corresponding to the mean elements of asteroid 3996 1988 XG_1. At the end of the integrated evolution, the eccentricity has been pumped to a very high value (greater than 0.9). The inclination also shows relatively large oscillations. At this point our integration scheme gives spurious results, as discussed in the text.

tary orbits with that of Laskar (1988). We have observed minor changes, mainly due to a small difference in the value of the g_6 frequency and a much richer frequency spectrum in the evolution of Jupiter's and Saturn's orbits. However, no qualitative change was apparent in the results.

Having gained confidence in our integration scheme we are going to discuss, in the next two subsections, the results of two sets of runs performed with different samples of bodies crossing the ν_6 resonance as a consequence of the Yarkovsky effects. First, we use a sample of regolith-free bodies 5 to 20 m in size, both stony and iron-rich. In this case, as we discussed earlier (Sect. 2.2), the "seasonal" Yarkovsky effect is probably the dominant one and Eq. (11) can be used for the semimajor axis evolution. Secondly, we consider two populations of asteroidal fragments, 50 m and 1 m in radius, with regolith-like surface properties, and in this case we use Eq. (12) to model the dominant "diurnal" Yarkovsky effect.

3.2. Regolith-free bodies evolving under the "seasonal" effect

Fig. 7 shows the evolution of the mean orbital elements which is typical for this class of objects. We have chosen initial mean elements corresponding to asteroid 1981 WR, that is $a = 2.280061$ AU, $e = 0.0889699$, $i = 2^\circ.82532$ (from the Milani and Knežević database, see Milani et al. 1994). This asteroid is located more or less in the middle of the Flora region.

Panel (a) of the figure shows the secular semimajor axis decay, with a variable rate due to random changes in the obliquity γ. The time required to reach the resonance matches the time scale shown in Fig. 1. When the ν_6 resonance is crossed, the mean eccentricity [shown in panel (b)] undergoes a sudden increase, and then keeps oscillating around a mean value of about 0.62. Thanks to this high eccentricity, the mean inclination [shown in panel (c)] also undergoes large perturbations. The way the resonance crossing works in pumping up the eccentricity is shown clearly in Fig. 8: as the semimajor axis decreases, the topology of the level curves of the averaged Hamiltonian is drastically changed and the orbit is "dragged" from a low- to a high-eccentricity circulation of the critical argument through an intermediate phase of resonant libration around $\varpi - \varpi_6 = 180^\circ$. This behavior matches well the topology of the phase space at the ν_6 resonance according to the theory of Morbidelli and Henrard (1991, Fig. 1), which shows moderate-eccentricity librations around $\varpi - \varpi_6 = 180^\circ$ at mean inclinations between

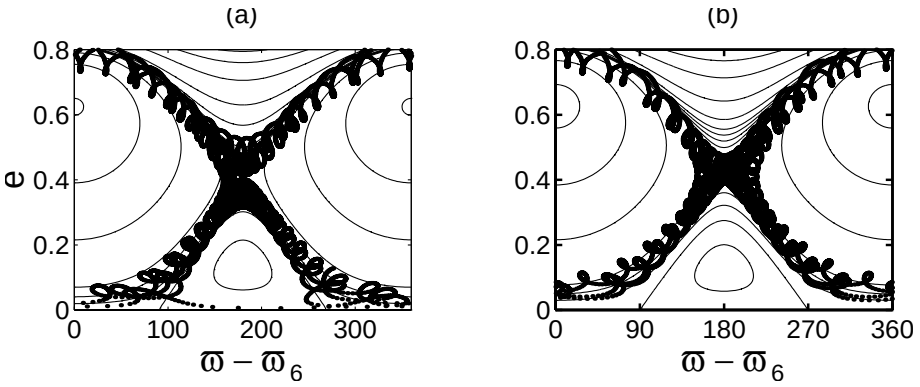

Fig. 11a and b The same as in Fig. 8 but for the orbital evolution shown in Fig. 10, near a time of rapid eccentricity growth [panel **a**] and decrease [panel **b**]. In either case the orbit switches from low- to high-eccentricity circulation or *vice versa*, without being captured in a libration zone.

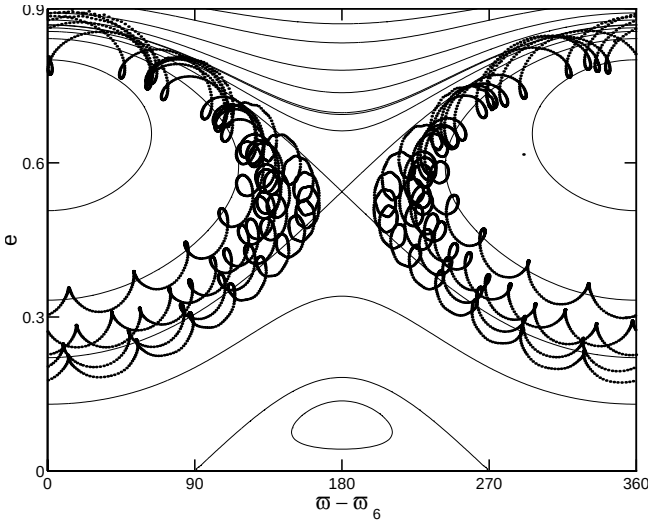

Fig. 12. The same as in Fig. 11 but for the interval preceding the end of the integration. Here the orbit gets trapped into a large-amplitude, high-eccentricity libration about $\varpi - \varpi_6 = 0$, which gradually shifts upwards as the semimajor axis is increased.

3° and 5°. Note that the integrated orbit follows only approximately the level curves, with "wiggles" caused by Jupiter's nonresonant perturbations. We have performed a large number of similar runs for both stony and iron bodies, and found in all cases the same kind of qualitative results, namely the transition to a high-eccentricity circulation mode after crossing the resonance.

Of course, the real orbital evolution is expected to be more complicated and should be investigated by using fully numerical integrations (we plan to do this in the next stage of our work on this issue). After crossing the ν_6 resonance, the fragments soon encounter the $4:1$ mean motion resonance with Jupiter and the ν_{16} secular resonance, and after this other resonances with the inner planets can affect the orbital elements in a significant way (Michel and Froeschlé 1997, Michel 1997). However, we believe that the most important result reported above – the effectiveness of the ν_6 resonance in pumping up the eccentricity of orbits crossing it under the Yarkovsky effect – is a robust one, and will be confirmed by more complex dynamical models. The same applies to the results described in the next subsection.

3.3. Regolith-covered bodies evolving under the "diurnal" effect

Fig. 9 shows an example of orbital evolution for a regolith-covered body 50 m in radius in the Flora region, under the effect of the "diurnal" Yarkovsky effect. The initial conditions correspond to the mean elements of asteroid (2580) Smilevskia ($a = 2.18255$ AU, $e = 0.19527$, $i = 0^\circ.32962$).

Panel (a) shows that the semimajor axis undergoes a random walk with varying slopes, corresponding to collisional changes in the obliquity. In two occasions the orbit crosses the resonance, and at these times the eccentricity undergoes sudden and drastic changes, and the inclination is also affected. In this particular case the eccentricity, after staying at high peak values for a few tens of Myr at the resonance crossings, returns to more or less the previous moderate (≈ 0.3) values when the orbit is driven back into the Flora region.

However, this is not always the case. Fig. 10 shows another example of the orbital evolution driven by the "diurnal" Yarkovsky effect. The initial conditions now correspond to the mean elements of asteroid 3996 1988 XG_1 ($a = 2.25933$ AU, $e = 0.103693$, $i = 0^\circ.89691$). Several features are similar to those of the previous case, but here at the end of the 400 Myr run the mean eccentricity exceeds 0.9, and after the first resonance crossing the orbit spends most of the time in the high-eccentricity state. We acknowledge that for such extreme values of the eccentricity the $15^{\rm th}$ degree truncation of the perturbing function in the asteroid's eccentricity adopted in our dynamical model (see Sect. 2.1) is certainly not sufficient to yield an accurate orbital evolution, and therefore we may get spurious results.

On the other hand, the same "phase space diagrams" we used in Fig. 8 are useful to understand the dynamical mechanisms at work in this case as well. Panels (a) and (b) of Fig. 11 correspond to two intervals of a few Myr centered at about 283 and 320 Myr after the beginning of the integration shown in Fig. 10, respectively. In the former case, the orbit passes directly from the low- to the high-eccentricity circulation mode, without being captured into a "libration island" as in the case of Fig. 8. Possibly this is simply due to the higher rate of the semimajor axis change in this case. The opposite happens in the panel (b) interval, when the eccentricity is rapidly decreased by the resonance crossing. Finally, Fig. 12 shows what happens just

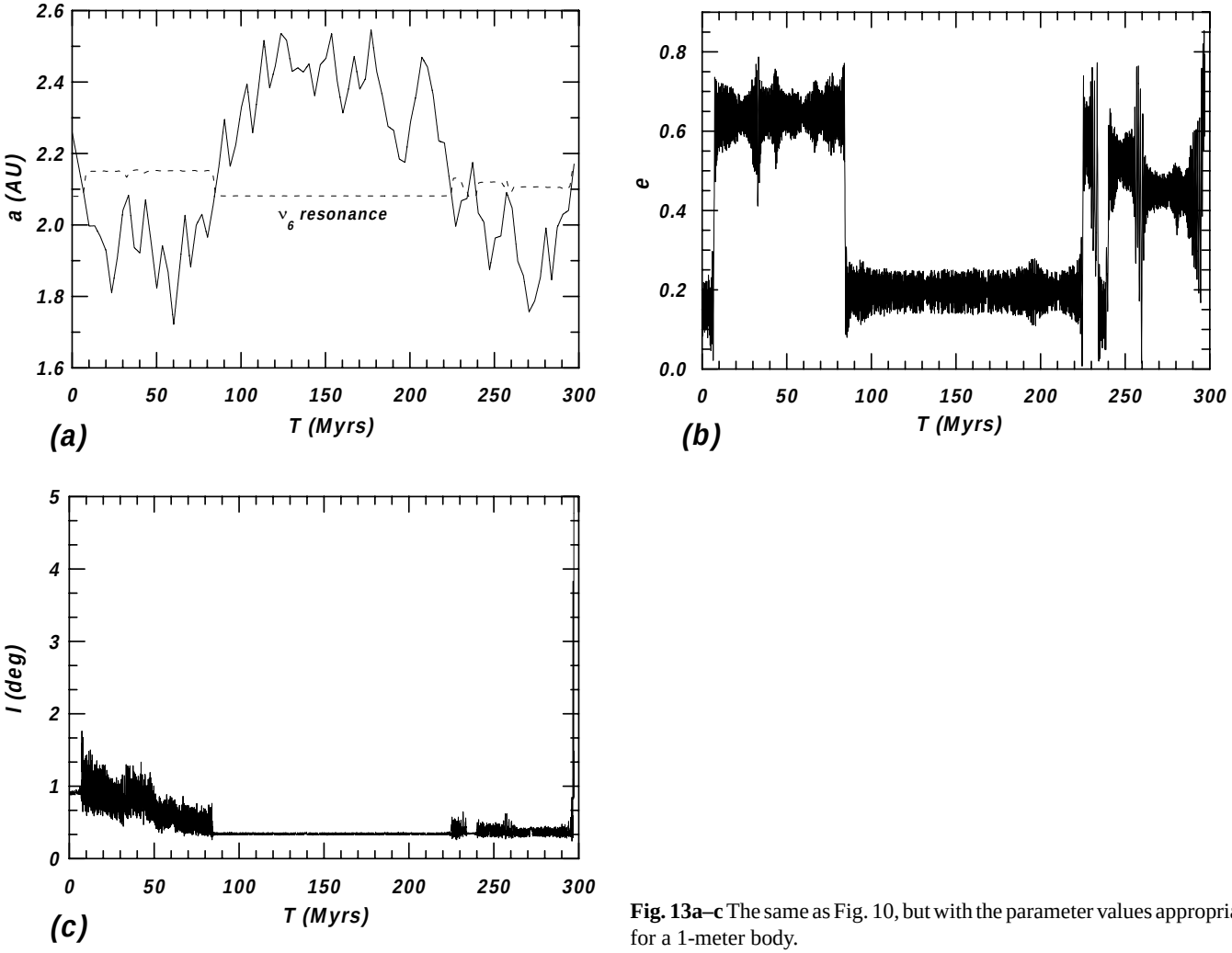

Fig. 13a–c The same as Fig. 10, but with the parameter values appropriate for a 1-meter body.

before the end of the evolution shown in Fig. 10: here the orbit gets trapped into a large-amplitude, high-eccentricity libration about $\varpi - \varpi_6 = 0$, which shifts to higher eccentricities as the semimajor axis grows due to the "diurnal" Yarkovsky effect (see Figs. 10a and 10b). Of course, this kind of mechanism should be explored by using a better dynamical model, maintaining a good accuracy at very high eccentricities.

Finally, Fig. 13 shows the result of an evolution starting from the same initial conditions used for Fig. 10 but taking the $\dot{a}_{max}$ and τ_{rot} value appropriate for a 1-meter body. The main difference with respect to Fig. 10 is that the time step for the random walk in semimajor axis is shorter. On the other hand, the behaviors of the eccentricity and the inclination are very similar to those of Fig. 10.

4. Conclusions

The main results of this paper can be summarized as follows:

1. We have estimated by numerical simulations the characteristic time scales for transporting asteroid fragments into the ν_6 resonance through diffusion of semimajor axes caused by the Yarkovsky effects. Regolith-free bodies 5 to 20 m in size can drift into the resonance through the "seasonal" semimajor axis decay within their collisional lifetime from a region of the inner asteroid belt of width ranging from several hundredths to a few tenths of AU, depending on the stony vs. metal-rich composition. Larger, 100-m sized bodies can also random walk into the resonance from the inner part of the Flora region provided their surface is covered by a thin regolith. For meter-sized bodies, the effectiveness of the "diurnal" Yarkovsky effect in changing their semimajor axis depends sensitively upon the thermal conductivity of their surface layer and their rotation rate. Further data on these physical properties are needed to assess whether or when the Yarkovsky effect is important in delivering them to the resonances.
2. The bodies whose orbital evolution is dominated by the "seasonal" version of the Yarkovsky effect always undergo large increases of eccentricity (enough for their orbits to become Earth-crossing) when they cross the resonance at semimajor axes ≈ 2.1 AU.
3. When the "diurnal" effect is the dominant one, the semimajor axis evolution has a random walk-like character, allowing these bodies to cross the ν_6 resonance in both senses; such

episodic resonance-crossing events are typically accompanied by large "jumps" in the eccentricity and lesser perturbations in the inclination. The Yarkovsky-driven evolution into ν_6 may explain the observed overabundance of "Small Earth Approachers" (SEAs) compared to larger near-Earth asteroids (Rabinowitz 1994, 1998). However, it seems unlikely that the subgroup of SEAs with $a \approx 1$ AU and small eccentricities (Rabinowitz et al. 1993, Bottke et al. 1996) can come from the main asteroid belt thanks to Yarkovsky effects, as proposed by Rubincam (1995). The reason is that according to our results the ν_6-crossing episodes always lead to large eccentricity increases (even disregarding other resonances), and the Yarkovsky force is not effective enough in circularizing the orbits while their semimajor axes are decreased (Rubincam 1998, Vokrouhlický and Farinella 1998). Of course Earth encounters could bring down the eccentricity, but this is not likely to occur frequently enough.

Further work on the issues addressed in this paper is needed in several directions. In particular, we plan to carry out fully numerical simulations of fragment orbits including the gravitational forces of both the outer and inner planets besides the Yarkovsky effects, and taking into account the stochastic obliquity changes related to impacts. As far as analytical models are concerned, it would be very useful to develop them, in analogy to what we have done here for ν_6, for the Jovian mean motion resonances, such as the 3:1 and 4:1 resonances which are probably very important for meteorite transport.

Acknowledgements. We dedicate this paper to the memory of Michèle Moons, who had kindly provided us with her algebraic manipulator MINIMS. We are grateful to B. Gladman, Z. Knežević, F. Marzari and A. Morbidelli (in his capacity as a reviewer) for useful comments and discussions. P.F. acknowledges support from the Italian Space Agency (ASI) and the Italian Ministry for University and Scientific Research (MURST).

References

Afonso G., R.S. Gomes, M.A. Florczak, 1995, Planet. Space Sci. 43, 787
Bottke W.F. Jr., M.C. Nolan, H.J. Melosh, A.M. Vickery, R. Greenberg, 1996, Icarus 122, 406
Brouwer D., G. Clemence, 1961, *Methods of Celestial Mechanics*, Academic Press, New York
Burns J.A., P.L. Lamy, S. Soter, 1979, Icarus 40, 1
Campo Bagatin A., A. Cellino, D.R. Davis, P. Farinella, P. Paolicchi, 1994, Planet. Space Sci. 42, 1079
Ceplecha Z., 1992, A&A 263, 361
Ceplecha Z., 1996, A&A 311, 329
Consolmagno J.C., D.T. Britt, C.P. Stoll, 1998, Meteoritics Planet. Sci., submitted
Dohnanyi J.W., 1969, J. Geophys. Res. 74, 2531
Duriez L., 1977, A&A 54, 93
Farinella P., R. Gonczi, Ch. Froeschlé, C. Froeschlé, 1993a, Icarus 101, 174
Farinella P., Ch. Froeschlé, R. Gonczi, 1993b, Celest. Mech. 56, 287
Farinella P., C. Froeschlé, R. Gonczi, 1994a, in *Asteroids Comets Meteors 1993* (A. Milani, M. Di Martino & A. Cellino, eds.), p. 205, Kluwer, Amsterdam
Farinella P., Ch. Froeschlé, C. Froeschlé, R. Gonczi, G. Hahn, A. Morbidelli and G.B. Valsecchi, 1994b, Nature 371, 314
Farinella, P., F. Marzari, D. Vokrouhlický, W.K. Hartmann, D.R. Davis, S.J. Weidenschilling, 1997, BAAS 29, 1045 (abstract)
Farinella P., D. Vokrouhlický, W.K. Hartmann, 1998, Icarus 132, 378
Froeschlé Ch., H. Scholl, 1987, A&A 179, 294
Froeschlé Ch., G. Hahn, R. Gonczi, A. Morbidelli, P. Farinella 1995, Icarus 117, 45
Gladman B.J., F. Migliorini, A. Morbidelli, V. Zappalà, P. Michel, A. Cellino, Ch. Froeschlé, H.F. Levison, M. Bailey, M. Duncan, 1997, Science 277, 197
Hagihara Y., 1971, *Celestial Mechanics*, Vol. II, MIT Press, Cambridge
Hamilton D.H., 1994, Icarus 109, 221
Hartmann W.K., P. Farinella, S.J. Weidenschilling, E.V. Ryan, D. Vokrouhlický, F. Marzari, D. Spaute, D.R. Davis, 1997, Lunar Planet. Sci. XXVIII, 517
Jopek T.J., P. Farinella, Ch. Froeschlé, R. Gonczi, 1995, A&A 314, 353
Knežević Z., 1986, Celest. Mech. 38, 123
Knežević Z., A. Milani, P. Farinella, Ch. Froeschlé, C. Froeschlé, 1991, Icarus 93, 316
Laskar J., 1985, A&A 144, 133
Laskar J., 1988, A&A 198, 341
Laskar J., 1991, in *Predicability, Stability, and Chaos in N-Body Dynamical Systems* (A.E. Roy, ed.), p. 93, Plenum Press, New York
Liou J.-C., H.A. Zook, 1997, Icarus 128, 354
Michel P., 1997, Icarus 129, 348
Michel P., Ch. Froschlé, 1997, Icarus 128, 230
Migliorini F., A. Morbidelli, V. Zappalá, B.J. Gladman, M.E. Bailey, A. Cellino, 1997, Meteoritics Planet. Sci. 32, 903
Milani A., M. Carpino, G. Hahn, A.M. Nobili, 1989, Icarus 78, 212
Milani A., E. Bowell, Z. Knežević, A. Lemaitre, A. Morbidelli, K. Muinonen, 1994, in *Asteroids Comets Meteors 1993* (A. Milani, M. Di Martino & A. Cellino, eds.), p. 467, Kluwer, Amsterdam
Moons M., 1991, *MINIMS: User's guide*, Rapport Interne No. 91/15 du Département de Mathématique FUNDP, Namur
Morbidelli A., 1993, Icarus 105, 48
Morbidelli A., J. Henrard, 1991, Celest. Mech. 51, 169
Morbidelli A., R. Gonczi, Ch. Froeschlé, P. Farinella, 1994, A&A 282, 955
Nobili A.M., A. Milani, M. Carpino, 1989, A&A 210, 313
Peterson C., 1976, Icarus 29, 91
Öpik E.J., 1951, Proc. Roy. Irish Acad. 54, 165
Rabinowitz D.L., 1994, Icarus 111, 364
Rabinowitz D.L., 1997, Icarus 127, 33
Rabinowitz D.L., 1998, Icarus 130, 275
Rabinowitz D.L., T. Gehrels, J.V. Scotti, R.S. McMillan, M.L. Perry, W. Wisniewski, S.M. Larson, E.S. Howell, B.E.A. Mueller, 1993, Nature 363, 704
Radzievskii V.V., 1952, Astron. Zh. 29, 162 (in Russian)
Rubincam D.P., 1995, J. Geophys. Res. 100, 1585
Rubincam D.P., 1998, J. Geophys. Res. 103, 1725
Scholl H., Ch. Froeschlé, 1991, A&A 245, 316
Šidlichovský M., 1989, Bull. Astron. Inst. Czechosl. 40, 92
Šidlichovský M., B. Melendo, 1986, Bull. Astron. Inst. Czechosl. 37, 65
Tagliaferri E., R. Spalding, C. Jacobs, S.P. Worden, A. Erlich, 1994, in *Hazards Due to Comets and Asteroids* (T. Gehrels, ed.), p. 199, University of Arizona Press, Tucson
Valsecchi G.B., A. Morbidelli, R. Gonczi, P. Farinella, Ch. Froeschlé, C. Froeschlé, 1995, Icarus 118, 169
Vokrouhlický D., P. Farinella, 1998, Astron J., submitted
Wetherill, G.W., 1980, Meteoritics 15, 386
Yomogida, K., T. Matsui, 1983, J. Geophys. Res. 88, 9513
Yoshikawa M., 1987, Celest. Mech. 40, 233